Building and Environment 282 (2025) 113314

Contents lists available at ScienceDirect

Building and Environment

journal homepage: www.elsevier.com/locate/buildenv

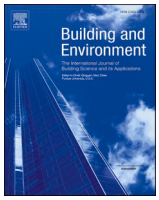

Performance of a prototype of the push-pull type personalized air curtain (PPAC) aimed to reduce respiratory infection risks

Narae Choi [a,*], Mariya Petrova Bivolarova [b], Pawel Wargocki [b]

[a] Department of Architectural Engineering, Graduate School of Engineering, The University of Osaka, 2-1 Yamadaoka, Suita, Osaka, Japan
[b] International Centre for Indoor Environment and Energy, Department of Environmental and Resource Engineering, Technical University of Denmark, Koppels Alle 402, 2800 Kongens Lyngby, Denmark

ARTICLE INFO

Keywords:
Personalized ventilation
Air cleaner
Infection risk
Airborne disease transmission

ABSTRACT

We present a prototype of the desktop-mounted push-pull personalized air curtain (PPAC) system. The system comprises a supplying unit and a capturing unit, which together create a lateral air barrier between an infector and an infectee. This air barrier is designed to block, entrain, and capture infectious aerosols generated during respiratory activities in close proximity.

The performance of the PPAC was examined in the office mock-up with a breathing thermal manikin and a heated cylinder, simulating two individuals sitting face-to-face at an 80 cm distance. The room was ventilated using either mixing or displacement ventilation, each supplying 20 L/s of clean outdoor air. A tracer gas was dosed into the exhaled air of the manikin to emulate infectious aerosol, and its concentration was measured at multiple locations to estimate the system's performance. The PPAC was tested at varying distances from the breathing manikin and with different airflow rates, while the manikin exhaled at different flow rates to simulate various aerosol releases.

When the PPAC was used, tracer gas concentration reduced considerably. The estimated capture efficiency reached nearly 60 %, comparable to the performance of some personal protective equipment. Capture efficiency improved with higher PPAC airflow rate and when the system was placed closer to the infector.

Further developments of the PPAC are necessary to understand its performance using actual aerosols. Still, our results show the considerable potential of using this type of solution for reducing infection risks in buildings with mostly sedentary occupants, such as schools and open-plan offices.

1. Introduction

The COVID-19 pandemic brought unprecedented disruptions to daily life worldwide and emphasized the critical need to reduce infection risks in indoor environments. Pathogens such as the Severe Acute Respiratory Syndrome Coronavirus-2 (SARS-CoV-2) causing COVID-19 are primarily transmitted via virus-laden droplets and aerosols released during human expiratory activities like breathing, speaking, sneezing, and coughing [1]. While larger droplets (>10 μm) deposit fairly quickly onto surfaces, smaller aerosols can remain airborne for minutes to hours [2–4], especially in poorly ventilated spaces, significantly increasing transmission risk. Therefore, controlling airborne aerosols indoors has been in focus as one of the effective infection prevention strategies.

Ventilation effectively reduces airborne transmission by diluting and removing infectious contaminants from indoor spaces [5,6]. Guidelines from the World Health Organization (WHO) [7], as well as documents from the Federation of European Heating, Ventilation, and Air Conditioning Associations (REHVA) [8] and ASHRAE [9], emphasize the importance of adequate ventilation rates to reduce exposure to airborne pathogens. Mixing ventilation (MV), commonly used in many indoor spaces, reduces aerosols' levels across the entire room but is less effective in reducing their concentration in the close proximity of the infected person [6]; it is usually called a short-range and is defined to be at a distance of below 1.5–2 m from the infected person. Liu et al. [10] reviewed previous studies, conducted both measurements and simulations and observed a significant increase in contaminant concentration within 1–1.5 m of an infected individual.

Other ventilation solutions have also been studied for their ability to maintain low levels of airborne pathogens. For example, displacement ventilation (DV) provides clean air in the lower part of a room. It removes aerosols using the thermal plume principle [11–14], which is

* Corresponding author.
E-mail address: choi@arch.eng.osaka-u.ac.jp (N. Choi).

https://doi.org/10.1016/j.buildenv.2025.113314
Received 12 February 2025; Received in revised form 26 May 2025; Accepted 19 June 2025
Available online 20 June 2025

Abbreviations

CU	Capturing unit of the PPAC
DU	Device uncertainty
DV	Displacement ventilation
MV	Mixing ventilation
SEM	Standard error of the mean
SU	Supplying unit of the PPAC
TU	Total experimental uncertainty
PAC	Personalized air curtain
PE	Personal exhaust
PPAC	Push-pull type personalized air curtain
PPE	Personal protective equipment
PV	Personal ventilation

Symbols

C_{CU}	Mean N_2O concentration at the exhaust of the PPAC capturing unit
C_{ex}	Mean N_2O concentration at the exhaust of the room ventilation
C_i	Mean N_2O concentration at measurement point i
C_{ref}	Mean N_2O concentration at measurement point i in the reference case
D_P	Horizontal distance between the manikin and the center of the PPAC
ε	Concentration reduction rate
η	Capture efficiency of the PPAC
n	Number of data
σ	Standard deviation
T_{F1100}	Air temperature at F1100
T_e	Exhaust air temperature of the background ventilation
T_s	Supply air temperature of the background ventilation
T_{SU}	Supply air temperature of the supplying unit
TU_{CU}	Total uncertainty of the mean concentration at exhaust of the PPAC capturing unit
TU_{ex}	Total uncertainty of the mean concentration at exhaust of the room ventilation
TU_{ref}	Total uncertainty of the mean concentration at the corresponding measurement point in the reference case
TU_i	Total uncertainty of the measurement point in the case under consideration
U_ε	uncertainty of the calculated capture efficiency
U_η	Uncertainty of the calculated concentration reduction rate
Q_{exh}	Exhalation rate
Q_P	Airflow rate of the PPAC
Q_v	Airflow rate of the room ventilation
S1100	Short range measuring point at 1100 mm height from the floor
S1700	Short range measuring point at 1700 mm height from the floor
F600	Farther distance measuring point at 600 mm height from the floor
F1100	Farther distance measuring point at 1100 mm height from the floor
F1700	Farther distance measuring point at 1700 mm height from the floor

considered more effective than using the MV. However, when exhaled aerosols are locked up near breathing height due to high emission speed and interference from thermal plumes, the DV systems can become less or even completely ineffective than MV [15–17]. Alternative ventilation strategies, such as impinging jet ventilation [18] and stratum ventilation [19,20], have also shown potential for higher efficiency compared to MV systems. Still, room-scale ventilation alone often falls short in controlling the exposure in the short-range, where close proximity results in high concentrations of infectious aerosols before they are diluted [21].

Localized strategies, such as personal ventilation (PV) and local exhaust, have been explored to enhance protection in close-contact situations, i.e., when the risk of exposure to aerosols in the short-range is high. PV provides clean air directly to the breathing zone, reducing short-range exposure to exhaled contaminants [6,22–24]. However, the effectiveness of PV is influenced by variables such as background ventilation, relative orientation of its users, and airflow interaction, which can sometimes increase infection risk [25–29]. Xu et al. [26] found that when an infected individual uses PV, the PV airflow can interact with the infector's exhaled airflow, increasing the exposure for others. Similarly, Liu et al. [28] reported that PV reduces infection risk in back-to-back orientations (65 % reduction with a 9 L/s PV supply) but performs worse than without PV in side-by-side setups. Local exhaust, which captures contaminants near the source, is particularly effective when the emission source is identifiable, such as in the medical consulting rooms [30,31] and dental clinics [32]. However, their performance also depends on parameters like exhaust outlet placement, airflow rate, and background ventilation [30,31,33]. A study combining PV and personal exhaust (PE) [34] found that using only PE to target an infector's exhaled contaminants is more effective (achieving an exposure reduction rate of over 70 % under MV, 80 % under DV) than using only PV to supply clean air to a susceptible individual (over 50 % under MV, less than 30 % under DV); when both PV and PE were used, the exposure reduction reached nearly 80 % with MV and more than 80 % with DV. Despite these benefits, challenges such as installation costs and difficulties integrating these systems into existing setups create limiting factors for the broader application of PV and PE.

In addition to ventilation-based strategies, several methods can be adopted without significant system installation, offering practical and cost-effective solutions for reducing transmission risks. Personal protective equipment (PPE), such as masks, was widely adopted during the pandemic [35]. High-efficiency masks, including N95 (95 % filtration for particles ≥0.3 μm, National Institute for Occupational Safety and Health (NIOSH) 42 CFR 84) and FFP2 (94 % filtration for particles ≥0.3 μm, EN149:2001+A1:2009), effectively block respiratory droplets and aerosols exhaled by infected individual or inhaled by a healthy individual, thereby reducing both emission and inhalation of infectious particles [36–39]. However, prolonged mask use can cause discomfort, particularly in settings requiring continuous wear [40,41]. Physical partitions could offer another solution by creating a physical barrier between individuals, limiting direct droplet transmission [42–44]. Ren et al. [42] found that partitions at least 60 cm in height are required to block contaminants effectively, and with appropriate ventilation, these barriers can reduce infection risk by up to 72 %. Personal air curtains (PAC) provide an innovative approach by creating an airflow barrier around an individual that protects the breathing zone from contaminants without obstructing visibility or communication. Xu et al. [45,46] investigated a PAC with upward airflow and demonstrated exposure reduction rates of up to 87 %, depending on factors such as PAC air velocity, distance from individuals, and emission velocity. Chen and Hao [47] examined a PAC with side airflow and reported exposure reductions of 55–80 %. Despite their potential, both physical barriers and air curtains generally only block aerosols without removing them, allowing infectious pathogens to disperse within the room, especially when the conditions and setup cause them to be less effective, which would typically be the case in practical applications in buildings compared with the laboratory experiments controlling in detail for

potentially influencing factors.

Using local exhaust in combination with a personalized air curtain can be a solution for reducing the dispersion of airborne contaminants. Melikov et al. [48] proposed a novel bed ventilation system, called the Hospital Bed Integrated Ventilation Cleansing Unit (HBIVCU). In this system, an additional air supply outlet was used to help direct the infectious contaminants from the patient toward a local exhaust. The performance of the HBIVCU was evaluated through both experiments [48] and CFD simulations [49], and the results showed that it could reduce the spread of gaseous contaminants from a lying patient. However, this system was specifically designed and tested for use in hospital beds, not for setting where occupants are seated. Takamure et al. [50] introduced a desktop air curtain system (DACS) featuring both discharge and suction ports with downward airflow, showing its blocking potential through visualization; however, no quantitative analysis was conducted.

To address the limitations of existing PAC systems and to create an effective solution for reducing the infectious aerosols at the source, i.e., in the close proximity of the seated infected person in shared indoor environments, we present in this paper a prototype of a novel personalized air curtain with push-pull side airflow (PPAC). The solution is designed to combine a localized directional air supply and exhaust functions to achieve enhanced contaminant control (Fig. 1). The paper presents measurements of the effectiveness of the PPAC in mitigating the risk of infection in the short-range when the room is ventilated by the mixing and displacement ventilation which are the most prevalently used in the buildings. The tests included the performance of the PPAC in capturing infectious aerosols under different operational conditions. The tracer gas was used to emulate aerosols exhaled by an individual, and we used breathing thermal manikin. The tests were done in the mock-up of the office space.

2. Methodology

2.1. Experimental setup

The experiment was conducted in a full-scale experimental chamber with dimensions of 1670 mm (width) × 4720 mm (length) × 2580 mm (height). Fig. 2 illustrates the experimental arrangement, simulating two individuals seated and facing each other. A thermal manikin representing a female body, 1.7 m in height, was put on a chair in a seating position, dressed in a t-shirt, trousers, underwear, socks, and shoes, corresponding to a clothing insulation value (clo) of 0.5. The manikin consisted of 18 body segments, each with individually controlled surface temperatures to maintain conditions corresponding to thermal comfort. The average heat output from the manikin across all cases was 56.3 W/m^2 (range: 53.4–58.7 W/m^2). The manikin was used to simulate the index case (the infector). In front of it, a metal heated cylinder (diameter: 250 mm, height: 800 mm) was placed at a distance of 80 cm to simulate a susceptible individual (the infectee). The heat was set up to generate approximately 70 W to replicate human thermal output.

In the mixing ventilation setup, clean air was supplied via a ceiling-mounted swirl diffuser (220 mm × 220 mm) with 12 openings. For displacement ventilation, a semicircular diffuser (duct diameter: 125 mm, width: 250 mm, height: 710 mm) served as the supply inlet; to adapt the diffuser to the low airflow rate, half of its inlet was covered. In both setups, a perforated ceiling-mounted circular diffuser was used as an exhaust. Although the locations of supply and exhaust can affect the contaminant distribution in the room [51–54], their positions were kept constant across all experimental conditions to focus on evaluating the basic performance of the PPAC. The supply was placed near the infector and the exhaust the infectee to create a more challenging condition for contaminant removal.

Dinitrogen oxide (N_2O) was used as a tracer gas to simulate airborne infectious aerosols. Tracer gas has been used in many previous studies to assess airborne transmission risk [55–57]. Although tracer gas cannot replicate physical phenomena such as evaporation and sedimentation, it has been proven to be able to reliably simulate the small expiratory droplet nuclei (<5 μm) [58,59], which are less influenced by these factors. These small particles represent a significant portion of exhaled droplet nuclei [60,61], remain airborne for extended periods [2–4], and are known to carry higher viral loads than larger droplets [62]. Therefore, tracer gas was adopted in this study to evaluate the effectiveness of the system in reducing airborne transmission risk. N_2O was added to the air exhaled by the manikin at a rate of 0.1 SLPM (standard liters per minute). Continuous breathing from the mouth was simulated via artificial lungs connected to the manikin.

A prototype of a desktop-sized personalized air curtain (PPAC) was placed on the table (735 mm in height) between the manikin and the heated cylinder (Fig. 3). The PPAC consisted of two components: an air supply unit (supplying unit), which created an airflow barrier to shield the exhaled aerosols, and a capturing unit, which removed aerosols blocked by and entrained into the barrier created by the air curtain. Each unit was 150 mm in width, 150 mm in length, and 600 mm in height. The dimensions of the inlet and outlet on both units were 30 mm (width) × 580 mm (height), and the units faced each other across a distance of 700 mm. The PPAC's inlet size was selected based on the study by Chen and Hao [47], which investigated the effectiveness of a personalized air curtain (PAC) in mitigating airborne transmission risk between two close individuals. Their study evaluated PAC performance using three different supply air velocities and inlet widths, all with 600 mm height. The results indicated that a velocity of 1 m/s with a 30 mm width condition significantly reduced infection risk compared to the other two conditions with higher velocities and reduced widths. Therefore, a 30 mm inlet width was adopted for the PPAC prototype.

In practical applications, air exhausted by the capturing unit of PPAC would be filtered and recirculated through the inlet of the supplying unit. In the present experiment, clean air was supplied to the supplying unit's inlet while the air exhausted from the capturing unit's outlet was

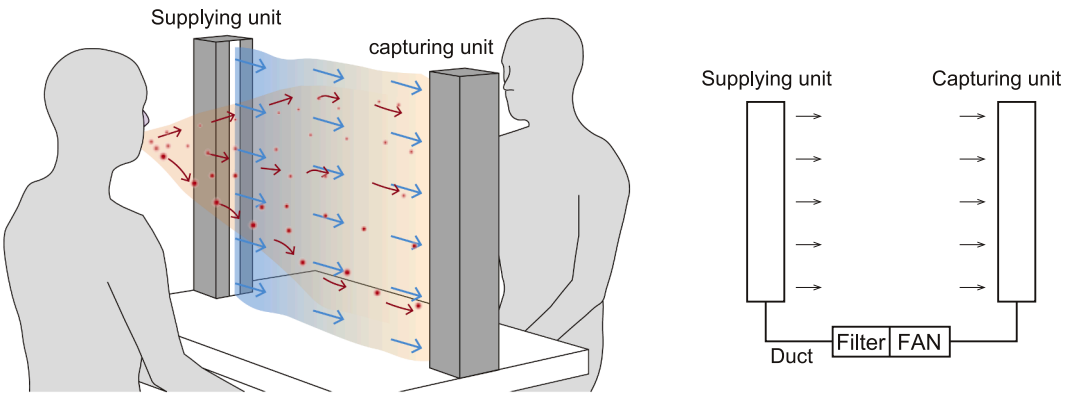

Fig. 1. The Concept of PPAC.

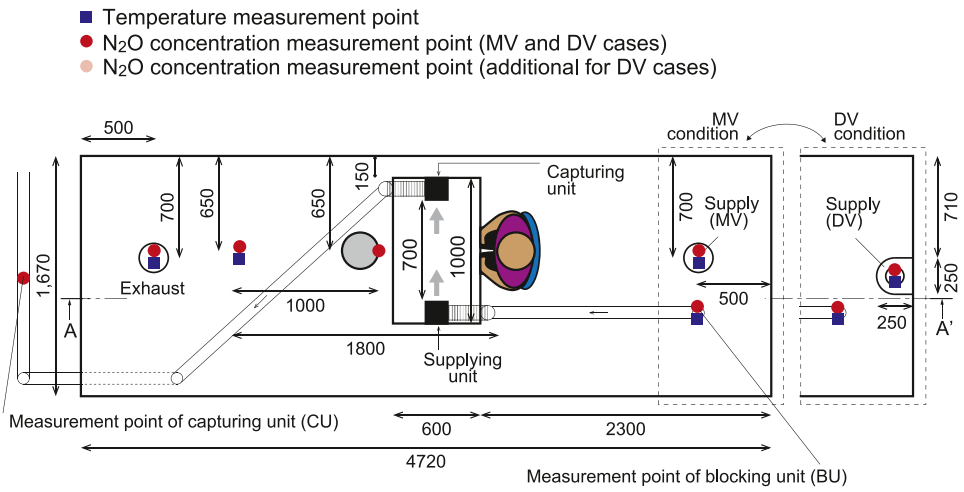

(a) Plan view of experimental chamber

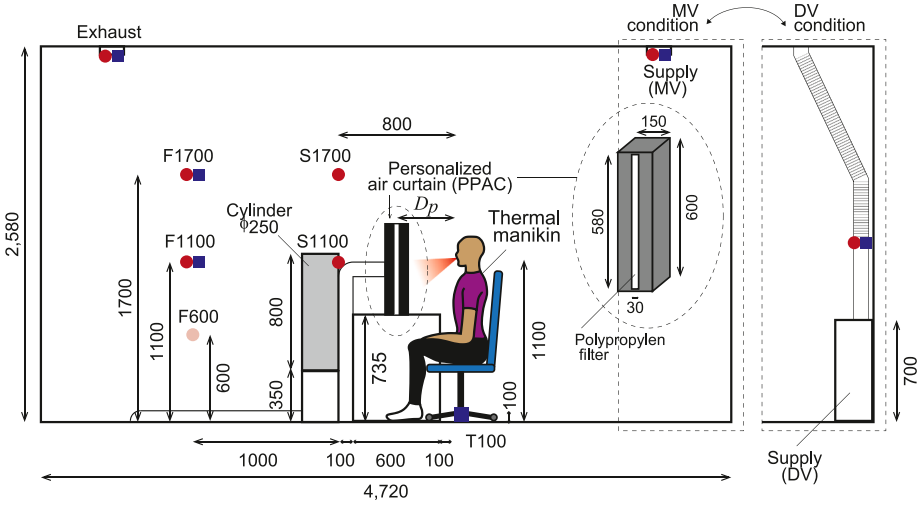

(b) Section view of experimental chamber

Fig. 2. Experimental setup and location of measuring points.

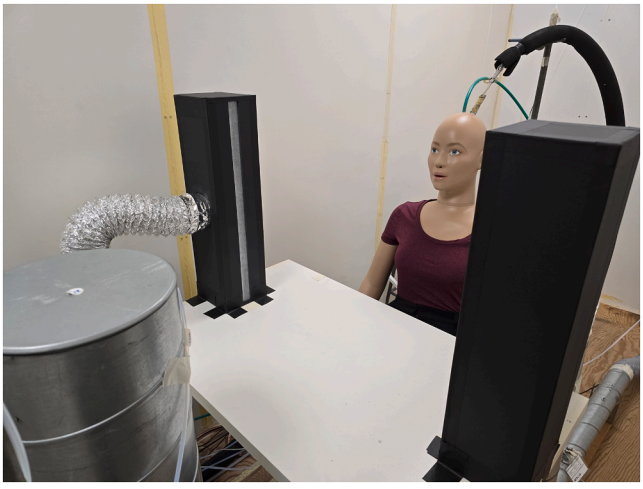

Fig. 3. Photo of the experimental setup.

extracted from the chamber. Polypropylene filters were installed at the inlet and outlet to produce a stable air screen with laminar airflow between the two units.

2.2. Measurements

The temperature and N_2O concentration measuring points are depicted in Fig. 2(a) and (b). To evaluate personal exposure for a seated individual at close proximity, N_2O concentration was measured at a height of 1100 mm, positioned 1 cm from the heated cylinder, simulating the susceptible individual (noted as S1100). An additional measurement point was placed at the same horizontal location but at a height of 1700 mm to represent the breathing height of a standing individual (noted as S1700). To investigate room air concentrations, N_2O was also measured 1800 mm away from the manikin at heights of 1100 mm (noted as F1100) and 1700 mm (noted as F1700). In the case of displacement ventilation (DV), an additional height was included, 600 mm (noted as F600), to observe vertical contaminant stratification.

The concentrations of N_2O in the air extracted from the chamber and through the exhaust unit of PPAC were measured; the concentration of N_2O in the air supplied to the chamber and the supplying unit of PPAC was measured at the beginning of each experimental condition tested.

N_2O concentrations at all measurement points were measured using a

photoacoustic multi-gas analyzer (GASERA ONE) with an accuracy of ±2 % of the reading. After reaching steady-state conditions, 20 measurements were taken and logged for each measuring location. It took approximately 190 min to complete this measurement in the room and the room's exhaust air.

Room air temperature and relative humidity were measured at F600, F1100, and F1700. Additionally, the temperature at the thermal manikin's ankle height, i.e., 100 mm (noted as T100), was recorded to examine vertical temperature gradients. Supply and exhaust temperatures for the background ventilation, as well as the supply temperature for the PPAC supplying unit, were also logged. Measurements were taken every minute using a bandgap temperature sensor (Sensirion SHT31) with an accuracy of ±0.2 °C.

2.3. Experimental conditions

The experimental conditions are presented in Table 1 and Fig. 4.

The measurements were made with mixing (MV) and displacement (DV) ventilation in operation, one at a time. The ventilation rate was set to 20 L/s, so assuming that the manikin and heated cylinder represent two individuals, it was 10 L/s per person. For comparison, ASHRAE standard 62.1 [63] specifies minimum outdoor airflow rates of approximately 15 cfm/person (7.1 L/s), and ASHRAE standard 241 [64] recommends 20 L/s per person for controlling infectious aerosols in many locations. In contrast, the World Health Organization (WHO) recommends 10 L/s per person [7]. The airflow rates of the PPAC's supplying and capturing units were tested at 10 L/s and 20 L/s, referred to as PPAC10 and PPAC20. These values were chosen based on the WHO guideline (10 L/s per person; and 20 L/s for two persons), as well as airflow levels tested in previous studies. Chen and Hao [47] evaluated PAC performance with supply air velocities of 1,2, and 3m/s, and found that 1 m/s performed best when the contaminant emission velocity was 1 m/s. In our setup, the calculated inlet velocities of the supplying unit were 0.56 m/s for PPAC10 and 1.11 m/s for PPAC20. Air velocity was measured at 15 points across the inlet surface the supplying unit to confirm the stability and distribution of the supply airflow. The results showed that the airflow was relatively uniform and had low turbulence intensity (See Appendix A).

To examine the influence of the PPAC's proximity to the contaminant source on blocking and capturing performance, two horizontal distances between the PPAC and thermal manikin (the infector) were tested: 400 mm, which placed the PPAC at the table's centerline and 200 mm, representing a closer distance between the thermal manikin's mouth and the center of the PPAC.

The thermal manikin continuously exhaled air at 14.4 L/min (default), corresponding to 6 L/min of air being exhaled over 2.5 s during a 6-*sec* breathing cycle if transient breathing was simulated [65]. Additional exhalation rates of 7.2 L/min and 20 L/min were tested to investigate the PPAC's performance at different tracer gas concentrations to simulate different aerosol emissions and the exhaled airspeed. Given the thermal manikin's mouth cross-sectional area of 158 mm^2, the exhaled air velocity was approximately 0.76 m/s at 7.2 L/min, 1.52 m/s at 14.4 L/min, and 2.11 m/s at 20 L/min.

The temperature of air supplied to the room was controlled to maintain a target room temperature of 23.5 °C, ensuring stable thermal conditions during all tests (see Appendix B). The average surface temperature of the individual segments of the manikin was 33.3 °C, ranging from 31.2 to 34.6 °C. The supply air temperature of the PPAC's supplying unit was also adjusted to match the room air temperature as closely as possible. This adjustment aligns with a real PPAC system, where the airflow would be recirculated and thus maintain the same temperature as the surrounding air.

Table 1
Experimental conditions (MV = Mixing ventilation; DV = Displacement ventilation; PPAC10 / PPAC20 = PPAC with an airflow rate of 10 L/s or 20 L/s, respectively; Qexh = Exhalation rate; low-Qexh / high-Qexh = Reduced or increased exhalation flow rate from the infector; "closer" in the case name indicates a condition in which the PPAC is positioned nearer to the infector than in the default configuration).

Condition (acronym), refer to Fig. 4 for illustration	Room ventilation		PPAC		Exhalation rate by the manikin Q_{exh} [L/min]
	Type	Airflow (supply and exhaust) Q_v [L/s]	Airflow (blocking and capturing units) Q_P [L/s]	Distance between manikin and PPAC D_P [mm]	
MV (Reference case)	MV	20	–	–	14.4
MV-low-Qexh	MV	20	–	–	7.2
MV-PPAC10	MV	20	10	400	14.4
MV-PPAC10-low-Qexh	MV	20	10	400	7.2
MV-PPAC10-closer	MV	20	10	200	14.4
MV-PPAC20	MV	20	20	400	14.4
MV-PPAC20-high-Qexh	MV	20	20	400	20
MV-PPAC20-closer	MV	20	20	200	14.4
DV (Reference case)	DV	20	–	–	14.4
DV-PPAC10	DV	20	10	400	14.4
DV-PPAC20	DV	20	20	400	14.4
DV-PPAC20-closer	DV	20	20	200	14.4

2.4. Analysis of the data

For each measurement point in each condition tested, twenty tracer gas concentration measurements were made, and the mean and standard deviation concentrations were calculated based on these measurements. The statistical variability and measurement device's accuracy were considered to quantify the experimental uncertainty.

The standard error of the mean (SEM) was calculated to estimate the precision of the mean concentration using the following equation:

$$SEM = \frac{\sigma}{\sqrt{n}} \tag{1}$$

where σ is the standard deviation of 20 measured data and n is the number of measurements ($n = 20$).

In addition to the statistical uncertainty, the measurement device used in this study had an accuracy of ±2 %, introducing systematic uncertainty. This device uncertainty (DU) was calculated as 2 % of the mean concentration. The total experimental uncertainty (TU) was determined by combining the statistical uncertainty (SEM) and the device uncertainty (DU):

$$TU = \sqrt{(SEM)^2 + (DU)^2} \tag{2}$$

To evaluate the performance of the PPAC, the capture efficiency (η), which is defined as the ratio of contaminants captured by the PPAC to the total contaminants removed from the room, was calculated using the following equation:

$$\eta = \frac{C_{CU} \cdot Q_P}{C_{ex} \cdot Q_v + C_{CU} \cdot Q_P} \tag{3}$$

In this equation, C_{CU} represents the mean tracer gas concentration measured at the capturing unit of the PPAC, while C_{ex} represents the mean tracer gas concentration at the exhaust of the room ventilation. Q_P denotes the airflow rate of the PPAC, and Q_v refers to the airflow rate of the room ventilation.

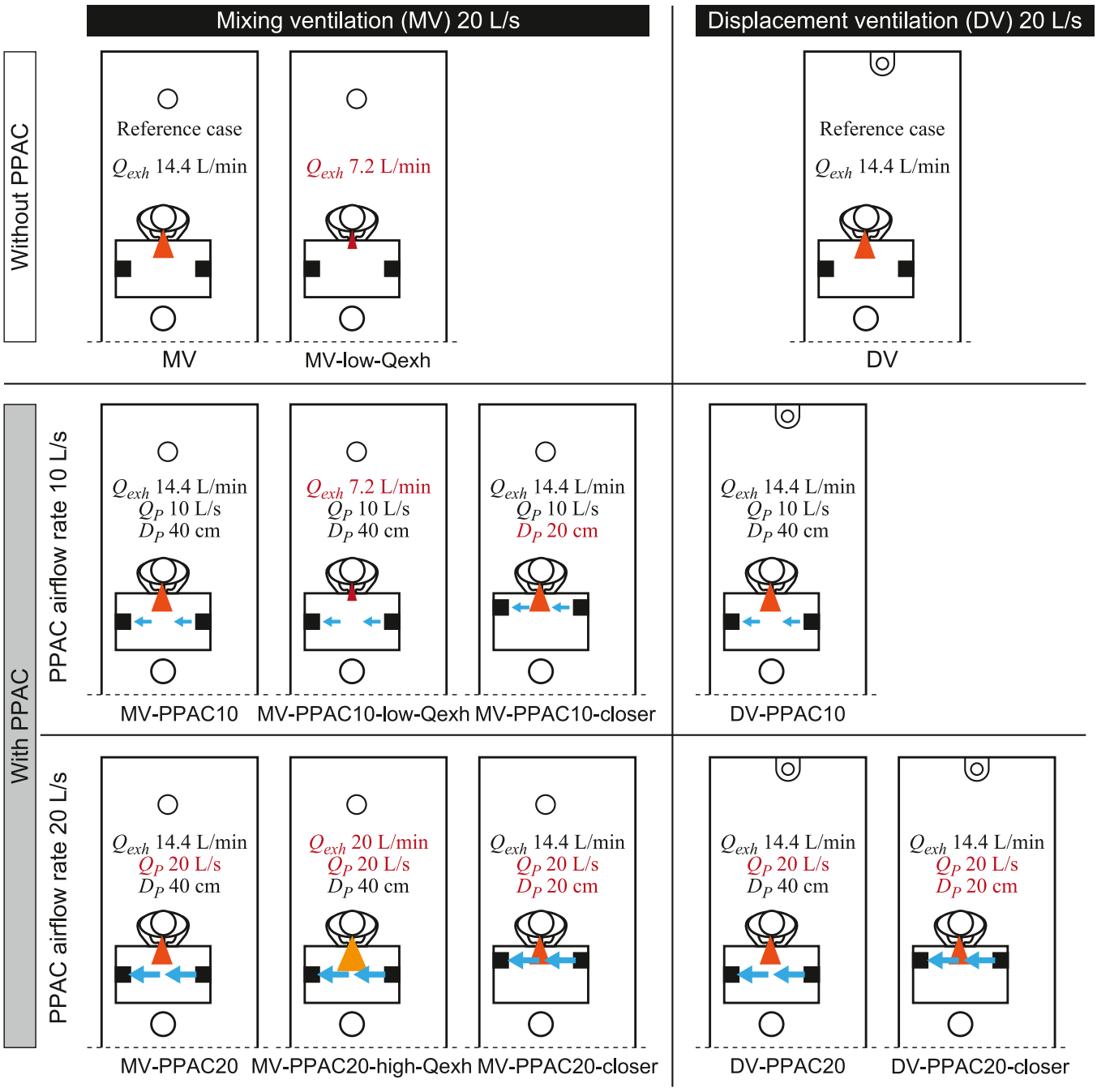

Fig. 4. Experimental conditions; Q_{exh} - exhalation rate, Q_P - PPAC airflow rate, D_P -horizontal distance between the manikin and centerline of the PPAC.

The uncertainty of the calculated capture efficiency (U_η) was calculated using the following:

$$U_\eta = \sqrt{\left(\frac{\partial \eta}{\partial C_{CU}} \cdot TU_{CU}\right)^2 + \left(\frac{\partial \eta}{\partial C_{ex}} \cdot TU_{ex}\right)^2} \quad (4)$$

Where TU_{CU} is the total uncertainty of the mean concentration at the capturing unit, and TU_{ex} is the total uncertainty of the mean concentration at the exhaust of the room ventilation. For this calculation, the uncertainty of the airflow rates was assumed to be negligible.

In addition to the capture efficiency, the concentration reduction performance of the PPAC was evaluated at both short distance and far field from the infector. The contaminant concentration reduction rate (ε) [39,45] was calculated at each measurement point relative to the reference case using the following equation:

$$\textit{Reduction rate } \varepsilon = \frac{C_{ref} - C_i}{C_{ref}} \quad (5)$$

Here, C_{ref} represents the mean tracer gas concentration at measurement point i in the reference case without the PPAC, while C_i represents the mean tracer gas concentration at measurement point i in the case under consideration.

For the analysis, the conditions with mixing ventilation (MV) and the conditions with PPAC were compared to those without PPAC. For the analysis, the conditions with displacement ventilation (DV) and the conditions with PPAC were compared to those without PPAC.

To calculate the uncertainty of the calculated reduction rate ε (U_ε), following equation was used:

$$U_c = \sqrt{\left(\frac{\partial \varepsilon}{\partial C_i} \cdot TU_i\right)^2 + \left(\frac{\partial \varepsilon}{\partial C_{ref}} \cdot TU_{ref}\right)^2} \quad (6)$$

Where TU_{ref} is the total uncertainty of the mean concentration at the corresponding measurement point in the reference case, and TU_i is the total uncertainty of the measurement point in the case under consideration.

3. Results

3.1. Tracer gas measurements

The calculated mean N_2O concentrations and their corresponding errors as described in 2.4 at each measuring point for each condition that was tested, are presented in Fig. 5. The results indicate that tracer gas concentrations in cases when the PPAC was in use were lower than when it was not present, simply demonstrating the PPAC's ability to block and capture the air exhaled by thermal manikin.

In the condition with mixing ventilation (MV) without the PPAC (Case MV), the concentration at S1700 was slightly higher than at other measuring points. However, concentrations at four measurement points and the exhaust were nearly uniform in the case with a lower emission speed (Case MV-low-Qexh). This indicates that higher emission speed is more likely to result in elevated short-range concentrations. When the PPAC was used under the same emission speed, the concentrations at S1100, S1700, F1100, and F1700 were nearly the same, implying that the PPAC effectively removed the contaminants before they dispersed near the cylinder, thereby preventing localized high concentrations.

In the condition when displacement ventilation (DV) was used without the PPAC (Case DV), the tracer gas concentration at S1100 was lower than when mixing ventilation (MV) was used without PPAC (Case MV), likely because of the thermal plume generated around the heated cylinder. The concentration at F600 was also low, reflecting the vertical concentration stratification typical of DV. However, the concentration at F1100 was as high as at the exhaust. In DV, a contaminant interface layer typically forms at the stratification height, where the upward convective airflow balances the supply airflow [11]. The relatively low background ventilation rate in this experiment likely caused the

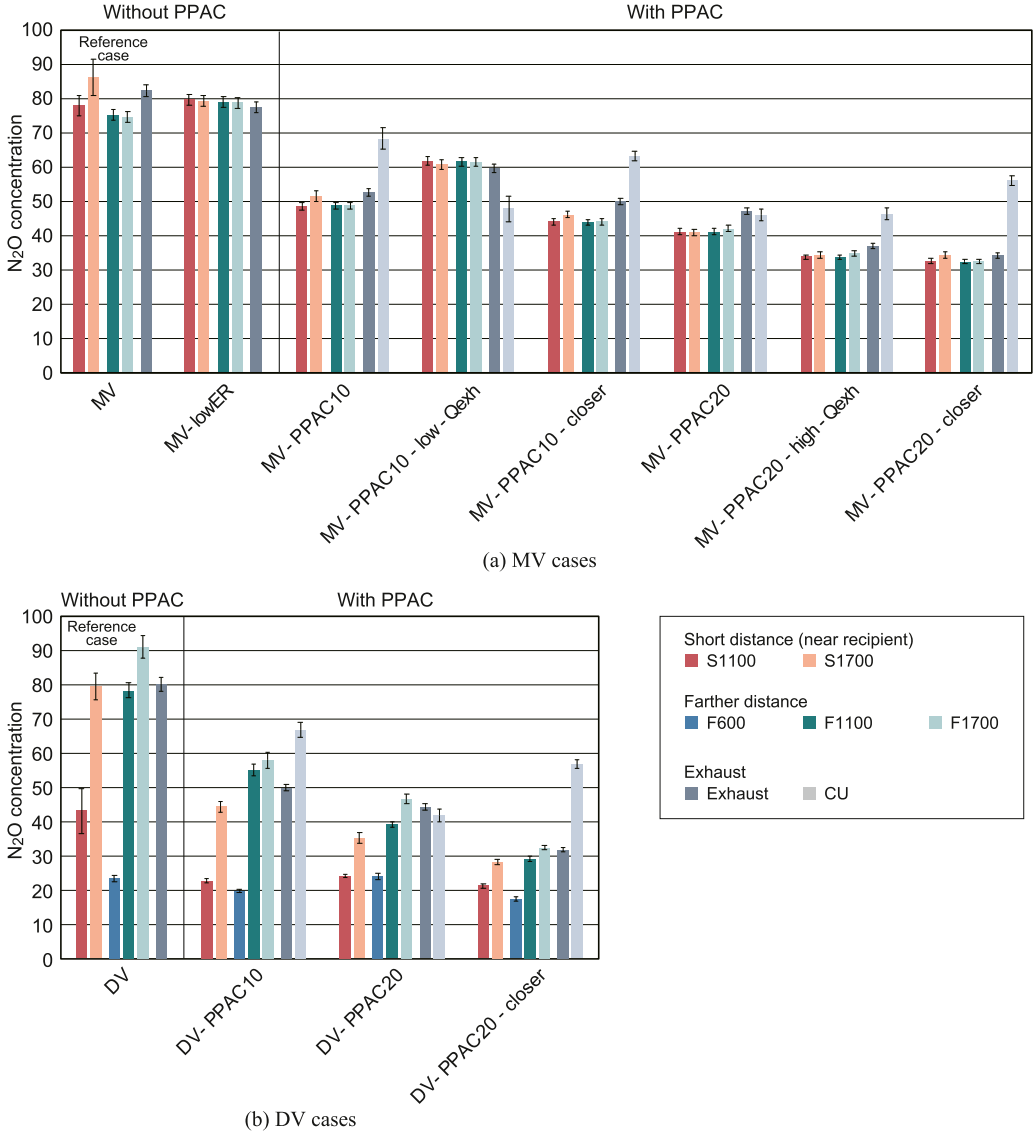

Fig. 5. Mean concentration of the tracer gas (N_2O) in conditions with mixing ventilation (MV), a, and displacement ventilation (DV), b; the bars indicate errors. MV = Mixing ventilation; DV = Displacement ventilation; PPAC10 / PPAC20 = PPAC with an airflow rate of 10 L/s or 20 L/s, respectively; low-Qexh / high-Qexh = Reduced or increased exhalation flow rate from the infector; "closer" in the case name indicates that the PPAC is placed nearer to the infector than in the default setup.

interface layer to form below 1100 mm. The concentration at F1700 in Case DV was higher than in Case MV and even exceeded the exhaust concentration, indicating that contaminants appeared to be locked up in the upper part of the room. Although DV reduced short-range concentrations, it posed a risk of creating locally higher concentration zones than Case MV. When the PPAC was used under DV, concentrations decreased at all measurement points, suggesting that the PPAC performed effectively in DV conditions as well. The PPAC did not significantly influence the concentrations at F600 because this point was below its height. Similar to DV without the PPAC, lower concentrations near the heated cylinder and in the lower part of the room were also observed when the PPAC was used. This suggests that the air barrier of the PPAC did not significantly disrupt the stratified environment created by DV.

3.2. Capture efficiency of PPAC (η)

The calculated capture efficiencies, obtained using Eq. (3) are shown in Fig. 6 for each tested condition. Capture efficiency is commonly used to evaluate the performance of local exhaust systems [30,31,66]. In this study, it is defined as the ratio of contaminants captured by the PPAC system to the total amount of contaminants removed from the room. We adopted this metric to quantify the effectiveness of the PPAC in removing exhaled contaminants without relying on reference case data, and to enable comparison with previously proposed local exhaust systems.

When the PPAC was set to an airflow rate of 10 L/s and positioned 40 cm from the emission source (thermal manikin), it captured nearly 40 % of contaminants under both MV and DV conditions (Case MV-PPAC10 and Case DV-PPAC10). At this airflow rate, the capture efficiency remained unchanged when the PPAC was placed closer to the manikin (Case MV-PPAC10-close). Doubling the PPAC airflow rate to 20 L/s increased the capture efficiency to nearly 50 % under both MV and DV conditions, though the improvement was not substantial (Case MV-PPAC20 and Case DV-PPAC). However, positioning the PPAC closer to the manikin further improved its performance, achieving capture efficiency up to nearly 60 %. These results suggest that close proximity to the emission source enhances system performance, especially at high PPAC airflow rates. The capture efficiency under MV and DV conditions did not differ significantly, indicating that the PPAC can perform effectively regardless of the room ventilation type.

The capture efficiency of the PPAC also varied with contaminant emission speed. The capture efficiency decreased at a lower emission speed (exhalation rate of 7.2 L/min; Case MV-PPAC10-low-Qexh). After being exhaled from the manikin, some contaminants would rise with the thermal plume around the manikin and spread into the room, whereas others may move forward in the exhalation direction while dispersing. Contaminants reaching the vicinity of the air barrier would be entrained and extracted by the capturing unit. However, at low exhalation speed, a more significant portion of the contaminants may have been more easily entrained in the plume of the manikin and dispersed into the room rather than being captured by the air barrier. Conversely, at a higher emission speed (20 L/min of exhalation rate; Case MV-PPAC20-high-Qexh), the capture efficiency increased compared to Case MV-PPAC20, possibly because the higher momentum allowed more contaminants to reach and be entrained by the air barrier. These findings suggest that the capture efficiency depends on the interplay between the exhalation rate (emission speed) and the PPAC airflow rate (air barrier speed). Furthermore, since emission speed was adjusted by varying the exhalation rate in this study, the contaminant concentration in the exhaled also changed. This variation in concentration could have further influenced the PPAC's contaminant removal efficiency.

3.3. Contaminant reduction effectiveness of PPAC (ε)

3.3.1. The effectiveness at the short distance (S1100, S1700)

The calculated concentration reduction rates, ε, obtained using Eq. (5) at S1100 and S1700 are shown in Fig. 7. In Case MV-PPAC10, the PPAC with 10 L/s airflow rate achieved a reduction rate of approximately 40 % at both S1100 and S1700 compared to Case MV without the PPAC, closely matching with the capture efficiency. When the PPAC was positioned closer to the contaminant source (Case MV-PPAC10-closer), the reduction rate at S1100 increased slightly to 45 %. Since the capture efficiency did not improve in this case, it is likely that while the air barrier blocked more exhaled contaminants at this closer position, it did not effectively capture them due to the low airflow rate of the PPAC. Case MV-PPAC20 showed higher effectiveness than Case MV-PPAC10, and placing the PPAC closer to the emission source (Case MV-PPAC20-closer) further enhanced the performance, achieving reduction rates of nearly 60 % at both S1100 and S1700, which also aligned with the capture efficiency. The high reduction rate at a short distance from the emission source suggests that the PPAC effectively removed exhaled

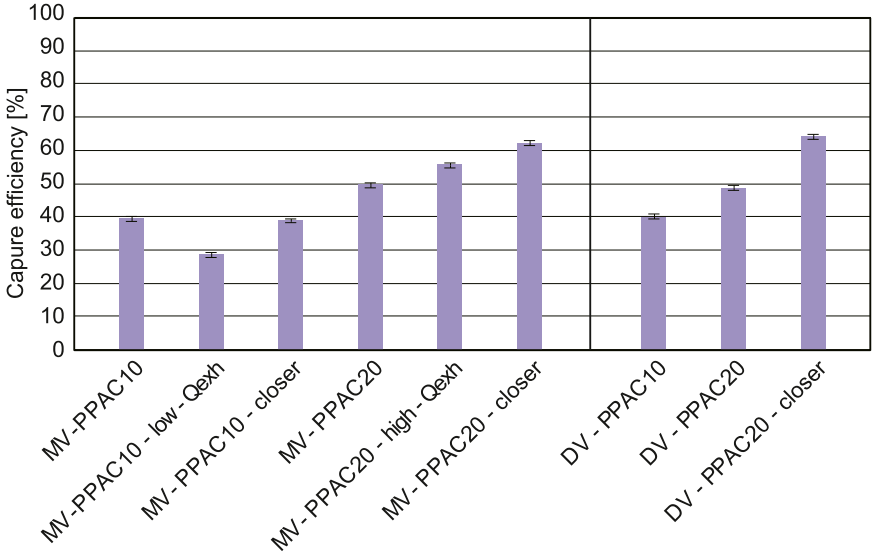

Fig. 6. Calculated capture efficiency of PPAC; the bars indicate errors. MV = Mixing ventilation; DV = Displacement ventilation; PPAC10 / PPAC20 = PPAC with an airflow rate of 10 L/s or 20 L/s, respectively; low-Qexh / high-Qexh = Reduced or increased exhalation flow rate from the infector; "closer" in the case name indicates that the PPAC is placed nearer to the infector than in the default setup.

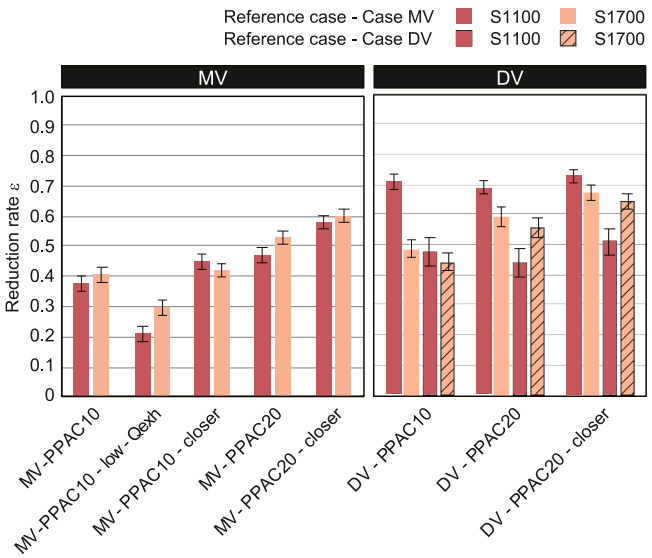

Fig. 7. Concentration reduction rate at S1100 and S1700; the bars indicate errors. MV = Mixing ventilation; DV = Displacement ventilation; PPAC10 / PPAC20 = PPAC with an airflow rate of 10 L/s or 20 L/s, respectively; low-Qexh / high-Qexh = Reduced or increased exhalation flow rate from the infector; "closer" in the case name indicates that the PPAC is placed nearer to the infector than in the default setup.

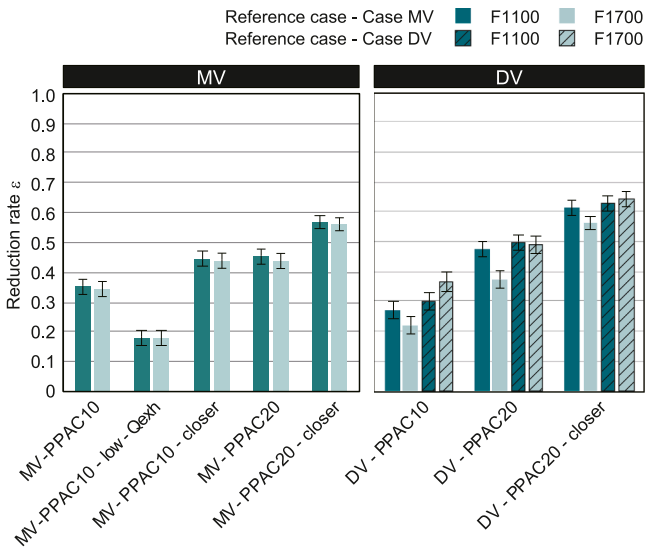

Fig. 8. Concentration reduction rate at F1100 and F1700; the bars indicate errors. MV = Mixing ventilation; DV = Displacement ventilation; PPAC10 / PPAC20 = PPAC with an airflow rate of 10 L/s or 20 L/s, respectively; low-Qexh / high-Qexh = Reduced or increased exhalation flow rate from the infector; "closer" in the case name indicates that the PPAC is placed nearer to the infector than in the default setup.

contaminants before they could disperse. Contaminant emission speed also influenced the reduction rate, following a similar trend to capture efficiency. When the emission speed was low, the reduction rate decreased.

For DV cases, reduction rates were calculated using both Case MV and DV without the PPAC as references. When the PPAC was used under DV, the concentration at S1100 was reduced by nearly 70 % compared to Case MV without the PPAC and by 45–50 % compared to Case DV without the PPAC. The removal efficiency at S1100 was relatively unaffected by the PPAC airflow rate or placement, possibly because this point was located in the convective boundary layer of the cylinder. At S1700, however, higher PPAC airflow rates and closer placement to the contaminant source improved the reduction rate. The highest performance was observed in Case DV-PPAC20-closer, achieving reduction rates of nearly 65 % at S1700 compared to Case MV and DV without the PPAC.

3.3.2. The effectiveness at farther distances (F1100, F1700)

The calculated reduction rates at F1100 and F1700 are depicted in Fig. 8. The reduction rates at F1100 and F1700 followed trends similar to those at S1100 and S1700, as well as the capture efficiency of the PPAC. The reduction rates increased with higher air flow rates and closer placement to the contaminant source under both MV and DV. The highest performance was also observed in Cases MV-PPAC20-closer and DV-PPAC20- closer. In MV-PPAC20- closer, the reduction rates were slightly below 60 % at F1100 and F1700 compared to Case MV without the PPAC. Similarly, in DV-PPAC20-d20, reduction rates reached nearly 60 % at both measurement points compared to Case DV without the PPAC. In MV cases, the reduction rates were relatively consistent between near and far locations due to the well-mixed air distribution. Conversely, DV cases showed more variability in reduction rates between measurement points, reflecting the influence of vertical stratification and horizontal concentration gradients inherent to displacement ventilation. Nonetheless, the PPAC showed the potential to reduce contaminant concentrations in the immediate vicinity of the source and at greater distances.

4. Discussion

Present measurements demonstrated that the proposed push-pull type personalized air curtain (PPAC) effectively captured exhaled contaminants and reduced contaminant concentration at both short and farther distances from the emission source. The PPAC showed comparable performance under mixing ventilation (MV) and displacement ventilation (DV) conditions, indicating that it can block and remove exhaled airborne contaminants without disrupting the existing air distribution. Its highest capture efficiency reached nearly 60 % when operating with an airflow of 20 L/s and positioned close to the emission source. These results confirm the PPAC's potential to reduce airborne transmission without requiring significant system installation.

In the experiment, clean air was provided through the supplying unit of the PPAC. The theoretical reduction rate for adding 20 L/s to the room ventilated with 20 L/s is 50 % at the exhaust. The PPAC's capture efficiency at 60 % is higher than this value, suggesting its more significant potential than simply increasing the ventilation rate. Moreover, since the capture efficiency may remain consistent under different ventilation rates, further investigations are needed to evaluate its performance across various background ventilation rates. Because the PPAC uses supplied air solely to create an air curtain immediately extracted by the capturing unit, the required air quality for the supplying unit should also be investigated to avoid unnecessarily using clean air.

As this is the first prototype, the 20 L/s airflow rate is a tentative value that achieved the best performance within the conditions in this experiment. This value could potentially be reduced through system optimization because the required flow rate will vary depending on the size and placement of the air barrier.

Previous studies on PV, PAC, partitions, and masks in a two-individual face-to-face setting are compared in Fig. 9. Unlike this study, which used tracer gas, those studies employed particle contaminants. Xu et al. [45] modeled high emission velocities (coughing at 12 m/s), while Ejaz et al. [39] simulated both breathing and coughing, with exhalation rates matching this study's breathing condition. While partitions and PACs reduce short-range infection risks by blocking contaminants emitted with high velocity, they do not remove them, allowing contaminants to disperse throughout the room. In contrast, personal air purifiers capture contaminants but have limited effective

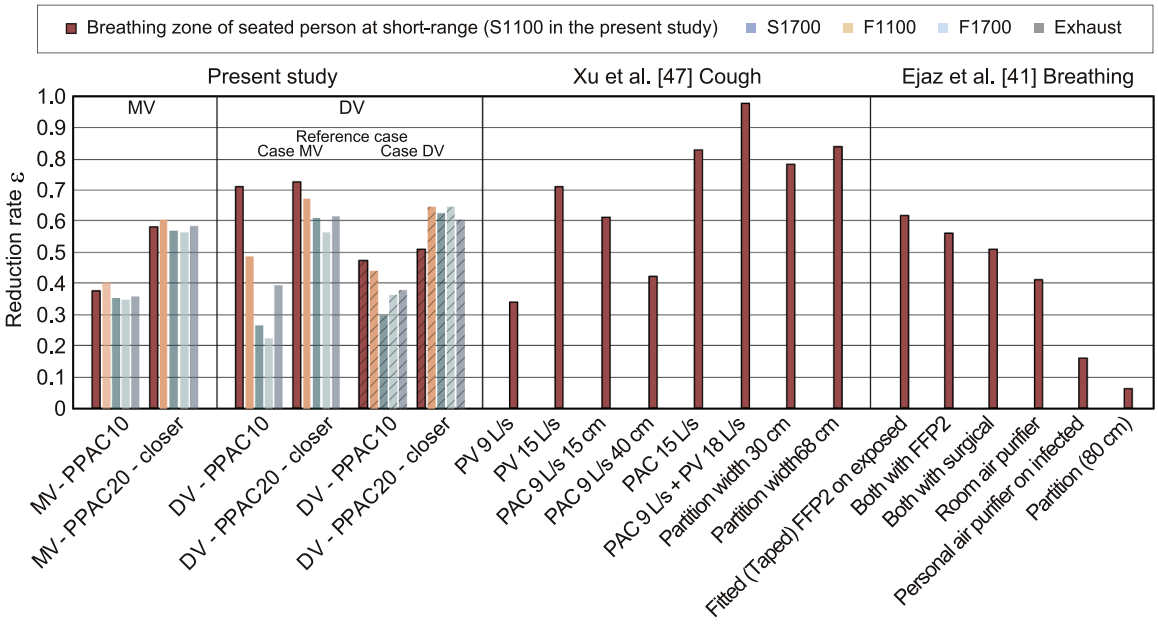

	Background ventilation	Contaminant emission and distance between infected person and recipient	Tested system		
			Type	Airflow rate [L/s]	Distance from healthy individual [cm]
Present study	MV, DV 20 L/s	Tracer gas (N2O) - Steady exhalation 14.4 L/min Distance - 80 cm	PPAC	10, 20	40, 60
Xu et al. [45]	MV 30.9 L/s	Particle (Simulated saliva solution) - Cough jet (12 m/s, 1 s three time with an interval of 5 s) Distance - 82 cm	PAC PV PAC+PV Partition	9, 15, 21, 27 9, 15, 21, 27 PAC 9 + PV 12 and 18 Height 51 cm	15, 40, 65 15, 40, 65 15, 40, 65
Ejaz et al. [39]	MV 36 L/s	Particle (Paraffin oil) - Breathing (Inhaling 2.5 s + pause 1 s + exhaling 2.5 s, exhalation 6 L/min) and cough (10 m/s, 1s 20 cough) Distance - 1.5 m	Facemasks (FFP2, surgical) Room air purifier Personal wearable purifier Partition (Height 40 and 80 cm)		

Fig. 9. Comparison of contaminant concentration reduction rates achieved by the PPAC and similar studies [41,47]. MV = Mixing ventilation; DV = Displacement ventilation; PV = Personalized ventilation; PAC = Personalized air curtain; PPAC10 / PPAC20 = PPAC with an airflow rate of 10 L/s or 20 L/s, respectively; "closer" in the case name indicates that the PPAC is placed nearer to the infector than in the default setup.

ranges. The push-pull type personalized air curtain system (PPAC) suggested in this study demonstrated removal efficiencies comparable to high-efficiency masks (FFP2) without the need for complex installations or physical barriers. However, the contaminant reduction effectiveness of the PPAC was lower than that of the PAC proposed in Xu et al.'s study (>80 %) [47] at short-distance. To optimize the PPAC system further, several limitations must be addressed.

When the PPAC is retrofitted for all occupants, it provides protection without the need to identify the infected individual. Since the PPAC captures exhaled contaminants near the emission source before they disperse, its relative risk reduction can be simply estimated based on its capture efficiency without requiring Wells-Riley equation calculations. Additionally, the PPAC can be used to remove general air pollutants when integrated with air filtration or air cleaning systems.

5. Limitations and future work

While the results demonstrated the potential of the PPAC, several limitations must be explored to further optimize its performance. In this study, the PPAC prototype used fixed inlet and outlet dimensions and a set distance between the blocking and capturing units. However, studies on physical barriers [44] suggest that barrier size significantly impacts blocking efficiency. Furthermore, the PPAC's inlet and outlet dimensions might not need to be identical. Future research should explore variations in these parameters to determine optimal configurations for different applications.

This study tested only two PPAC airflow rates (10 L/s and 20 L/s) and two horizontal distances between the manikin and PPAC. The results showed improved performance with higher PPAC airflow and close proximity to the source. However, the effectiveness of the system is likely influenced by the combined effects of supply airflow rate (velocity), the distance between the PPAC and the infector, and the release velocity of aerosol contaminants. Xu et al. [45] reported that system performance was more sensitive to distance when the PAC airflow rate was low, and that placing the system closer to either the infector or the infectee improved effectiveness. Previous studies using PAC [45–47] have also demonstrated that higher PAC airflow rate improves performance under stronger emissions (e.g., coughing) while lower airflow is effective for slower emissions. Since this study used a steady, low exhalation velocity (1.52 m/s), the PPAC should also be evaluated under stronger emissions such as coughing and sneezing. In such cases, a higher PPAC airflow rate may be required to prevent contaminants from

penetrating the air barrier. Alternatively, since exhalation velocity decreases with distance, placing the PPAC slightly farther from the source may improve interception without substantially increasing airflow. Future studies should investigate these variables in combination to identify optimal operating conditions.

The current PPAC prototype did not significantly disturb the vertical contaminant stratification typically observed in displacement-ventilated rooms. However, higher airflow rates of the PPAC may affect room air distribution more strongly. Future designs should aim to maintain a stable air barrier while minimizing disruption to the intended ventilation pattern.

Higher airflow rates may also raise practical concerns such as noise and vibration, which were not addressed in this study. It is important to optimize system configuration to avoid using unnecessarily high airflow rates, which could increase the noise generated by the fan. Future work should include noise measurements under various airflow conditions and explore design improvements that balance capture efficiency with acceptable sound levels.

While the PPAC is designed to block and capture infectious droplets and aerosols released during respiratory activities, this study used tracer gas to simulate airborne particles. Although tracer gas is commonly used to represent small aerosol particles (<5 μm), it does not account for the behavior of larger particles which are considerably affected by gravity and evaporation. However, because the PPAC is designed to operate in close proximity to the source, where larger particles are still suspended, it is expected to capture a portion of these particles before they deposit. Nonetheless, future studies should validate these results using actual particle generation in a recirculating PPAC setup to confirm its practical effectiveness across a broader range of particle sizes.

Room configuration is another important factor. The orientation of individuals relative to the PPAC may also influence its effectiveness. Previous studies [29,60] have shown that the orientation of individuals affects the performance of PV systems, particularly in side-by-side arrangements where PV systems are less effective. Similarly, the PPAC's performance may vary with different occupant orientations. The positions of ventilation inlet and outlet can also affect airflow patterns and the dispersion of exhaled contaminants [54]. In the current setup, the exhaust was located behind the susceptible person, and the inlet was near the infector, which likely created a less favorable condition for contaminant removal. In addition, in open-plan offices with partitioned workstations, physical dividers may help contain exhaled air around the infector and potentially enhance the PPAC's performance. These factors, including occupant orientation, ventilation layout, and the presence of partitions, should be further examined to better understand how they interact with the PPAC and influence its effectiveness.

6. Conclusion

This study presented the prototype of a push-pull type personalized air curtain (PPAC) and evaluated its effectiveness in removing exhaled airborne contaminants at both short and far distances. Experiments were conducted in a full-scale chamber under varying conditions, including two types of background ventilation (mixing ventilation (MV) and displacement ventilation (DV)), different PPAC airflow rates (velocities), and distances from the contaminant source. The air barrier generated by the PPAC effectively blocked and captured contaminants, substantially reducing personal exposure compared to cases without the PPAC. Based on the experimental results, the following conclusions can be drawn:

- The performance of the PPAC improved with a higher flow rate through the air curtain and closer proximity to the breathing manikin. At the PPAC airflow rate of 20 L/s and a distance of 20 cm from the breathing manikin, the capture efficiency was close to 60 % with mixing and displacement ventilation systems in the room mock-up compared to the conditions without the air curtain.
- The presented air curtain system effectively reduced contaminant concentrations close to the breathing manikin and farther away in the room, either with the mixing or displacement ventilation operating in the room mock-up, implying its considerable potential in reducing infectious aerosol exposure.
- With displacement ventilation, the contaminant concentrations in the lower part of the room were low, consistent with typical displacement ventilation characteristics. The PPAC enhanced contaminant removal in the room with displacement ventilation setup, achieving up to approximately 70 % compared to MV without the PPAC. However, room air concentrations under DV did not consistently show higher reduction rates than under MV, and the reasons need to be investigated.
- Future research should focus on optimizing system parameters, such as the size and airflow velocity of the air curtain, and experiments repeated with aerosols before the system can be considered for practical applications.

CRediT authorship contribution statement

Narae Choi: Writing – original draft, Methodology, Investigation, Funding acquisition, Formal analysis, Data curation, Conceptualization. **Mariya Petrova Bivolarova:** Writing – review & editing, Methodology, Investigation, Funding acquisition, Data curation. **Pawel Wargocki:** Writing – review & editing, Supervision, Project administration, Methodology, Funding acquisition, Conceptualization.

Declaration of competing interest

The authors declare the following financial interests/personal relationships which may be considered as potential competing interests:

Narae Choi reports financial support was provided by Japan Society for the Promotion of Science. Mariya Petrova Bivolarova, Pawel Wargocki reports financial support was provided by Fonden af 20. If there are other authors, they declare that they have no known competing financial interests or personal relationships that could have appeared to influence the work reported in this paper.

Acknowledgments

This work was supported by JSPS KAKENHI Grant Number 24K17405 (in Japan) and Fonden af 20. December (in Denmark).

Appendix A

Air velocity in the supply of PPAC supplying unit

The supply air velocity of the PPAC supplying unit was measured at 15 points, positioned 5 mm from the unit's surface. Measurements were conducted using a wireless omnidirectional thermal anemometer with a sampling rate of 8 Hz and an accuracy of ±0.02 m/s.

Fig. A presents the measured supply air velocity at the PPAC's supplying unit with the corresponding standard deviation (SD). Each value represents a 3-min average. The small SD values at all points indicate stable airflow. While there were some variations in air velocity, the differences were relatively minor. Table A summarizes the average air velocity and turbulence intensity across all measurement points. Given that the inlet surface area of the supplying unit was 0.0174 m^2, the measured velocity values closely aligned with the intended airflow rates of 10 L/s and 20 L/s. Turbulence

intensity was below 2 % for both airflow conditions, indicating a steady and controlled air distribution.

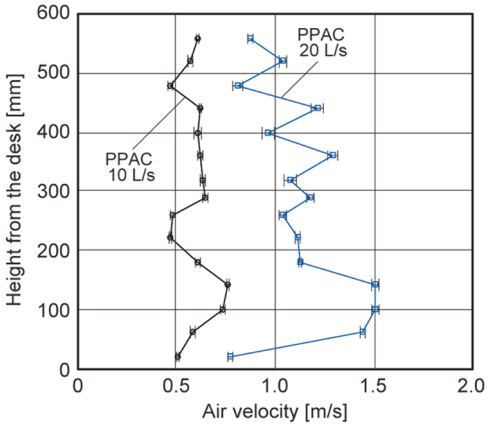

Fig. A. Measured air velocity with ±SD at the inlet of the supplying unit.

Table A
Average supply air velocity and turbulence intensity of the supplying unit.

	PPAC 10 L/s	PPAC 20 L/s
Average air velocity (standard deviation) [m/s]	0.59 (0.08)	1.13 (0.22)
Average turbulence intensity (standard deviation) [%]	1.88 (0.34)	1.89 (0.80)

Appendix B

Temperature

The measured temperatures are summarized in Table B. Each value represents the mean temperature recorded at each measurement point during a 15-minute logging period at the steady-state conditions. In the case of mixing ventilation (MV), room air temperatures were relatively uniform, suggesting well-mixed conditions. In contrast, when displacement ventilation (DV) was used, lower temperatures were measured near the floor (T100) compared to the upper part of the room, reflecting vertical stratification, as expected. The average temperature at F1100, which was averaged across all cases, was 23.7 °C (Min: 23.5 °C, Max: 24.2 °C). Although there were slight temperature variations between examined conditions, the differences were very small, and the target temperature was generally reached. The supply air temperature of the supplying unit was adjusted to match the room air temperature closely; the average temperature difference between the supplying unit and F1100 was 0.4 °C (Min: 0.2 °C, Max: 0.7 °C).

Table B
Measured temperatures.

Case	Ventilation		PPAC	T100 [°C]	F600 [°C]	F1100	F1700 [°C]	T_s-T_e [°C]	T_{BU}-T_{F1100} [°C]
	Supply T_s [°C]	Exhaust T_e [°C]	Supplying unit T_{SU} [°C]			T_{F1100} [°C]			
MV	19.2	24.2	23.6	23.5	23.7	23.6	23.7	−4.4	0.5
MV-low-Qexh	17.7	23.8	23.2	23.1	23.6	23.4	23.5	−5.5	0.3
MV-PPAC10	19.0	24.1	23.1	23.7	23.9	23.8	23.9	−4.1	0.3
MV-PPAC10-low-Qexh	18.0	23.9	23.2	23.4	23.7	23.6	23.7	−5.2	0.4
MV-PPAC10-closer	18.0	24.1	23.4	23.4	23.8	23.7	23.8	−5.4	0.4
MV-PPAC20	19.1	24.2	23.3	23.7	24.0	23.9	24.1	−4.2	0.3
MV-PPAC20-high-Qexh	18.5	23.7	23.0	23.2	23.6	23.4	23.5	−4.5	0.3
MV-PPAC20-closer	18.8	23.9	23.1	23.4	23.8	23.7	23.9	−4.4	0.2
DV	18.6	24.6	22.8	21.6	23.5	23.8	24.2	−4.2	0.7
DV-PPAC10	18.7	24.3	23.2	21.7	23.5	23.7	24.0	−4.4	0.7
DV-PPAC20	18.7	24.5	23.5	22.0	23.8	24.0	24.2	−4.8	0.6
DV-PPAC20-closer	18.9	24.5	23.3	21.9	23.8	23.9	24.2	−4.4	0.6

Data availability

No data was used for the research described in the article.

References

[1] C.C. Wang, K.A. Prather, J. Sznitman, J.L. Jimenez, S.S. Lakdawala, Z. Tufekci, L. C. Marr, Airborne transmission of respiratory viruses, Science 373 (2021) eabd9149, https://doi.org/10.1126/science.abd9149.

[2] J.P. Duguid, The size and the duration of air-carriage of respiratory droplets and droplet-nuclei, Epidemiol. Infect. 44 (1946) 471–479, https://doi.org/10.1017/S0022172400019288.

[3] L. Morawska, Droplet fate in indoor environments, or can we prevent the spread of infection? Indoor Air 16 (2006) 335–347, https://doi.org/10.1111/j.1600-0668.2006.00432.x.

[4] U. Ranga, SARS-CoV-2 aerosol and droplets: an overview, VirusDisease 32 (2021) 190–197, https://doi.org/10.1007/s13337-021-00660-z.

[5] Y. Li, G.M. Leung, J.W. Tang, X. Yang, C.Y.H. Chao, J.Z. Lin, J.W. Lu, P.V. Nielsen, J. Niu, H. Qian, A.C. Sleigh, H.-J.J. Su, J. Sundell, T.W. Wong, P.L. Yuen, Role of ventilation in airborne transmission of infectious agents in the built environment ? A multidisciplinary systematic review, Indoor Air 17 (2007) 2–18, https://doi.org/10.1111/j.1600-0668.2006.00445.x.

[6] A.K. Melikov, COVID-19: reduction of airborne transmission needs paradigm shift in ventilation, Build. Environ. 186 (2020) 107336, https://doi.org/10.1016/j.buildenv.2020.107336.

[7] Roadmap to Improve and Ensure Good Indoor Ventilation in the Context of COVID-19, 1st ed, World Health Organization, Geneva, 2021.

[8] REHVA COVID 19 GUIDANCE version 4.1, Federation of European Heating and Ventilation and Air Conditioning Associations (REHVA), 2021. https://www.rehva.eu/fileadmin/user_upload/REHVA_COVID-19_guidance_document_V4.1_15042021.pdf (accessed November 23, 2024).

[9] ASHRAE Positions on Infectious Aerosols, The American Society of Heating, Refrigerating and Air-Conditioning Engineers (ASHRAE), 2022. https://www.ashrae.org/File%20Library/About/Position%20Documents/PD_-Infectious-Aerosols-2022_edited-January-2023.pdf (accessed November 23, 2024).

[10] L. Liu, Y. Li, P.V. Nielsen, J. Wei, R.L. Jensen, Short-range airborne transmission of expiratory droplets between two people, Indoor Air 27 (2017) 452–462, https://doi.org/10.1111/ina.12314.

[11] M. Sandberg, C. Blomqvist, Displacement ventilation systems in office rooms, Displacement ventilation systems in office rooms, ASHRAE Trans 95 (2) (1989) 1041–1049.

[12] Y. Yin, W. Xu, J.K. Gupta, A. Guity, P. Marmion, A. Manning, B. Gulick, X. Zhang, Q. Chen, Experimental study on displacement and mixing ventilation systems for a patient ward, HVACR Res 15 (2009) 1175–1191, https://doi.org/10.1080/10789669.2009.10390885.

[13] L. Xiaoping, N. Jianlei, G. Naiping, Spatial distribution of human respiratory droplet residuals and exposure risk for the co-occupant under different ventilation methods, HVACR Res 17 (2011) 432–445, https://doi.org/10.1080/10789669.2011.578699.

[14] R. Kosonen (Ed.), Displacement Ventilation, REHVA, Brussels, Belgium, 2017.

[15] E. Bjørn, P.V. Nielsen, Dispersal of exhaled air and personal exposure in displacement ventilated rooms: dispersal of exhaled air and personal exposure in displacement ventilated rooms, Indoor Air 12 (2002) 147–164, https://doi.org/10.1034/j.1600-0668.2002.08126.x.

[16] Y. Li, P. Nielsen, M. Sandberg, Displacement ventilation In hospital environments, ASHRAE J 53 (2011) 86–88.

[17] N. Choi, T. Yamanaka, K. Sagara, Y. Momoi, T. Suzuki, Displacement ventilation with radiant panel for hospital wards: measurement and prediction of the temperature and contaminant concentration profiles, Build. Environ. 160 (2019) 106197, https://doi.org/10.1016/j.buildenv.2019.106197.

[18] L. Wang, X. Dai, J. Wei, Z. Ai, Y. Fan, L. Tang, T. Jin, J. Ge, Numerical comparison of the efficiency of mixing ventilation and impinging jet ventilation for exhaled particle removal in a model intensive care unit, Build. Environ. 200 (2021) 107955, https://doi.org/10.1016/j.buildenv.2021.107955.

[19] Z. Lin, J. Wang, T. Yao, T.T. Chow, Investigation into anti-airborne infection performance of stratum ventilation, Build. Environ. 54 (2012) 29–38, https://doi.org/10.1016/j.buildenv.2012.01.017.

[20] Y. Lu, M. Oladokun, Z. Lin, Reducing the exposure risk in hospital wards by applying stratum ventilation system, Build. Environ. 183 (2020) 107204, https://doi.org/10.1016/j.buildenv.2020.107204.

[21] P.V. Nielsen, C. Xu, Multiple airflow patterns in human microenvironment and the influence on short-distance airborne cross-infection – A review, Indoor Built Environ 31 (2022) 1161–1175, https://doi.org/10.1177/1420326X211048539.

[22] J. Pantelic, G.N. Sze-To, K.W. Tham, C.Y.H. Chao, Y.C.M. Khoo, Personalized ventilation as a control measure for airborne transmissible disease spread, J. R. Soc. Interface 6 (2009), https://doi.org/10.1098/rsif.2009.0311.focus.

[23] R. Cermak, A.K. Melikov, Protection of occupants from exhaled infectious agents and floor material emissions in rooms with personalized and underfloor ventilation, HVACR Res 13 (2007) 23–38, https://doi.org/10.1080/10789669.2007.10390942.

[24] E. Katramiz, N. Ghaddar, K. Ghali, D. Al-Assaad, S. Ghani, Effect of individually controlled personalized ventilation on cross-contamination due to respiratory activities, Build. Environ. 194 (2021) 107719, https://doi.org/10.1016/j.buildenv.2021.107719.

[25] X. Li, J. Niu, N. Gao, Co-occupant's exposure to exhaled pollutants with two types of personalized ventilation strategies under mixing and displacement ventilation systems, Indoor Air 23 (2013) 162–171, https://doi.org/10.1111/ina.12005.

[26] C. Xu, X. Wei, L. Liu, L. Su, W. Liu, Y. Wang, P.V. Nielsen, Effects of personalized ventilation interventions on airborne infection risk and transmission between occupants, Build. Environ. 180 (2020) 107008, https://doi.org/10.1016/j.buildenv.2020.107008.

[27] J. Xu, S. Fu, C.Y.H. Chao, Performance of airflow distance from personalized ventilation on personal exposure to airborne droplets from different orientations, Indoor Built Environ 30 (2021) 1643–1653, https://doi.org/10.1177/1420326X20951245.

[28] W. Liu, L. Liu, C. Xu, L. Fu, Y. Wang, P.V. Nielsen, C. Zhang, Exploring the potentials of personalized ventilation in mitigating airborne infection risk for two closely ranged occupants with different risk assessment models, Energy Build 253 (2021) 111531, https://doi.org/10.1016/j.enbuild.2021.111531.

[29] C. Xu, Y. Ren, N. Li, L. Liu, X. Mei, Y. Fan, Performance of personalized ventilation in mitigating short-range airborne transmission under the influence of multiple factors, Build. Simul. 16 (2023) 2077–2092, https://doi.org/10.1007/s12273-023-1035-z.

[30] J. Zong, C. Lin, Z. Ai, Performance of low-volume air cleaner and local exhaust in mitigating airborne transmission in hospital outpatient rooms, Phys. Fluids 36 (2024) 013342, https://doi.org/10.1063/5.0185630.

[31] J. Yoshihara, T. Yamanaka, T. Kobayashi, N. Choi, N. Kobayashi, Performance of combination of local exhaust system and floor-supply displacement ventilation system as prevention measure of infection in consulting room, Japan Architecture Review 6 (1) (2023) e12413, https://doi.org/10.1002/2475-8876.12413.

[32] J.R. Allison, C. Dowson, K. Pickering, G. Červinskytė, J. Durham, N.S. Jakubovics, R. Holliday, Local exhaust ventilation to control dental aerosols and droplets, J. Dent. Res. 101 (2022) 384–391, https://doi.org/10.1177/00220345211056287.

[33] J. Yang, C. Sekhar, D.K.W. Cheong, B. Raphael, A time-based analysis of the personalized exhaust system for airborne infection control in healthcare settings, Sci. Technol. Built Environ. 21 (2015) 172–178, https://doi.org/10.1080/10789669.2014.976511.

[34] J. Yang, S.C. Sekhar, K.W.D. Cheong, B. Raphael, Performance evaluation of a novel personalized ventilation–personalized exhaust system for airborne infection control, Indoor Air 25 (2015) 176–187, https://doi.org/10.1111/ina.12127.

[35] Z. Zhai, Facial mask: a necessity to beat COVID-19, Build. Environ. 175 (2020) 106827, https://doi.org/10.1016/j.buildenv.2020.106827.

[36] T. Jefferson, L. Dooley, E. Ferroni, L.A. Al-Ansary, M.L. Van Driel, G.A. Bawazeer, M.A. Jones, T.C. Hoffmann, J. Clark, E.M. Beller, P.P. Glasziou, J.M. Conly, Physical interventions to interrupt or reduce the spread of respiratory viruses, Cochrane Database Syst. Rev. (2023) 2023, https://doi.org/10.1002/14651858.CD006207.pub6.

[37] M. Abboah-Offei, Y. Salifu, B. Adewale, J. Bayuo, R. Ofosu-Poku, E.B.A. Opare-Lokko, A rapid review of the use of face mask in preventing the spread of COVID-19, Int. J. Nurs. Stud. Adv. 3 (2021) 100013, https://doi.org/10.1016/j.ijnsa.2020.100013.

[38] R. Mittal, K. Breuer, J.H. Seo, The flow physics of face masks, Annu. Rev. Fluid Mech. 55 (2023) 193–211, https://doi.org/10.1146/annurev-fluid-120720-035029.

[39] M.F. Ejaz, S. Kilpeläinen, S. Lestinen, R. Kosonen, Experimental comparison of structural and active protective methods against breath- and cough-borne aerosols in a meeting room, Build. Environ. 265 (2024) 111993, https://doi.org/10.1016/j.buildenv.2024.111993.

[40] Q. Zhong, J. Song, D. Shi, C.-H. Dung, Protective facemask-induced facial thermal stress and breathing burden during exercise in gyms, Build. Environ. 244 (2023) 110840, https://doi.org/10.1016/j.buildenv.2023.110840.

[41] X. Lang, N.G. Vasquez, W. Liu, D.P. Wyon, P. Wargocki, Effects of wearing masks indoors on the cognitive performance and physiological and subjective responses of healthy young adults, Build. Environ. 252 (2024) 111248, https://doi.org/10.1016/j.buildenv.2024.111248.

[42] C. Ren, C. Xi, J. Wang, Z. Feng, F. Nasiri, S.-J. Cao, F. Haghighat, Mitigating COVID-19 infection disease transmission in indoor environment using physical barriers, Sustain. Cities Soc. 74 (2021) 103175, https://doi.org/10.1016/j.scs.2021.103175.

[43] M. Mirzaie, E. Lakzian, A. Khan, M.E. Warkiani, O. Mahian, G. Ahmadi, COVID-19 spread in a classroom equipped with partition – A CFD approach, J. Hazard. Mater. 420 (2021) 126587, https://doi.org/10.1016/j.jhazmat.2021.126587.

[44] J. Bartels, C.F. Estill, I.-C. Chen, D. Neu, Laboratory study of physical barrier efficiency for worker protection against SARS-CoV-2 while standing or sitting, Aerosol Sci. Technol. 56 (2022) 295–303, https://doi.org/10.1080/02786826.2021.2020210.

[45] J. Xu, H. Guo, Y. Zhang, X. Lyu, Effectiveness of personalized air curtain in reducing exposure to airborne cough droplets, Build. Environ. 208 (2022) 108586, https://doi.org/10.1016/j.buildenv.2021.108586.

[46] J. Xu, C. Wang, H. Guo, Effect of personalized air curtain combined with mixing ventilation on dispersion of aerosols released at different velocities from respiratory activities during close contact, J. Build. Eng. 87 (2024) 109016, https://doi.org/10.1016/j.jobe.2024.109016.

[47] M. Chen, S. Hao, Numerical study on the cutting off performance of a novel personalized air curtain in a general consulting ward, Dev. Built Environ. 16 (2023) 100239, https://doi.org/10.1016/j.dibe.2023.100239.

[48] A. Melikov, Z. Bolashikov, E. Georgiev, Novel ventilation strategy for reducing the risk of airborne cross infection in hospital rooms, in: Proceedings of Indoor Air 2011, Austin, USA, 2011.

[49] W. Su, Z. Ai, A. Melikov, Potential of a bed ventilation system in reducing the risk of exposure to contaminants in infectious wards, J. Build. Eng. 84 (2024) 108525, https://doi.org/10.1016/j.jobe.2024.108525.
[50] K. Takamure, Y. Sakamoto, T. Yagi, Y. Iwatani, H. Amano, T. Uchiyama, Blocking effect of desktop air curtain on aerosols in exhaled breath, AIP Adv 12 (2022) 055323, https://doi.org/10.1063/5.0086659.
[51] Z. Lin, T.T. Chow, C.F. Tsang, K.F. Fong, L.S. Chan, CFD study on effect of the air supply location on the performance of the displacement ventilation system, Build. Environ. 40 (2005) 1051–1067, https://doi.org/10.1016/j.buildenv.2004.09.003.
[52] Y. Kang, Y. Wang, K. Zhong, Effects of supply air temperature and inlet location on particle dispersion in displacement ventilation rooms, Particuology 9 (2011) 619–625, https://doi.org/10.1016/j.partic.2010.05.018.
[53] J. Ren, Y. Wang, Q. Liu, Y. Liu, Numerical study of three ventilation strategies in a prefabricated COVID-19 inpatient ward, Build. Environ. 188 (2021) 107467, https://doi.org/10.1016/j.buildenv.2020.107467.
[54] N. Izadyar, W. Miller, Ventilation strategies and design impacts on indoor airborne transmission: a review, Build. Environ. 218 (2022) 109158, https://doi.org/10.1016/j.buildenv.2022.109158.
[55] Z. Ai, C.M. Mak, N. Gao, J. Niu, Tracer gas is a suitable surrogate of exhaled droplet nuclei for studying airborne transmission in the built environment, Build. Simul. 13 (2020) 489–496, https://doi.org/10.1007/s12273-020-0614-5.
[56] W. Zhao, S. Lestinen, M. Guo, S. Kilpeläinen, J. Jokisalo, R. Kosonen, An experimental study on airborne transmission in a meeting room with different air distribution methods, Build. Environ. 256 (2024) 111522, https://doi.org/10.1016/j.buildenv.2024.111522.
[57] W. Zhao, M.F. Ejaz, S. Kilpeläinen, J. Jokisalo, R. Kosonen, The potential of local exhaust combined with mixing and displacement ventilation systems to mitigate COVID-19 transmission risks, Build. Environ. 266 (2024) 112076, https://doi.org/10.1016/j.buildenv.2024.112076.
[58] M. Bivolarova, J. Ondráček, A. Melikov, V. Ždímal, A comparison between tracer gas and aerosol particles distribution indoors: the impact of ventilation rate, interaction of airflows, and presence of objects, Indoor Air 27 (2017) 1201–1212, https://doi.org/10.1111/ina.12388.
[59] Z.T. Ai, A.K. Melikov, Airborne spread of expiratory droplet nuclei between the occupants of indoor environments: a review, Indoor Air 28 (2018) 500–524, https://doi.org/10.1111/ina.12465.
[60] R.S. Papineni, F.S. Rosenthal, The size distribution of droplets in the exhaled breath of healthy Human subjects, J. Aerosol Med. 10 (1997) 105–116, https://doi.org/10.1089/jam.1997.10.105.
[61] C.Y.H. Chao, M.P. Wan, L. Morawska, G.R. Johnson, Z.D. Ristovski, M. Hargreaves, K. Mengersen, S. Corbett, Y. Li, X. Xie, D. Katoshevski, Characterization of expiration air jets and droplet size distributions immediately at the mouth opening, J. Aerosol Sci. 40 (2009) 122–133, https://doi.org/10.1016/j.jaerosci.2008.10.003.
[62] W.G. Lindsley, F.M. Blachere, R.E. Thewlis, A. Vishnu, K.A. Davis, G. Cao, J. E. Palmer, K.E. Clark, M.A. Fisher, R. Khakoo, D.H. Beezhold, Measurements of airborne influenza virus in aerosol particles from Human coughs, PLoS ONE 5 (2010) e15100, https://doi.org/10.1371/journal.pone.0015100.
[63] L. Damiano, D. Dougan, ANSI/ASHRAE Standard 62.1-2004, in: B. Capehart (Ed.), Encycl. Energy Eng. Technol. - 3 Vol. Set Print Version, CRC Press, 2007, pp. 50–62, https://doi.org/10.1201/9780849338960.ch6.
[64] ASHRAE, Standard 241, Control of Infectious Aerosols, American Society of Heating, Refrigerating and Air-Conditioning Engineers, Inc., Atlanta, GA, 2023.
[65] C.-E. Hyldgård, Humans As a Source of Heat and Air Pollution, Dept. of Building Technology and Structural Engineering, Aalborg, 1994.
[66] U. Madsen, N.O. Breum, P.V. Nielsen, Local exhaust ventilation—A numerical and experimental study of capture efficiency, Build. Environ. 29 (1994) 319–323, https://doi.org/10.1016/0360-1323(94)90029-9.